Regular Article

PHYSICAL CHEMISTRY RESEARCH
Published by the
Iranian Chemical Society
www.physchemres.org
info@physchemres.org

Phys. Chem. Res., Vol. 11, No. 3, 631-642, September 2023
DOI: 10.22036/pcr.2022.348858.2127

Combined Effects of Inclination Angle and Imposed Flow on Mixed Convective Cooling Inside a Vented Cavity Crossed by Nanofluids

I. Arroub[a,*], A. Bahlaoui[a], S. Belhouideg[a], A. Raji[b] and M. Hasnaoui[c]

[a]*Research Laboratory in Physics and Sciences for Engineers (LRPSI), Polydisciplinary Faculty, Sultan Moulay Slimane University, Béni-Mellal, Morocco*

[b]*Energy and Materials Engineering Laboratory (LGEM), Faculty of Sciences and Technics, Sultan Moulay Slimane University, Béni-Mellal, Morocco*

[c]*Laboratory of Fluid Mechanics and Energetics (LMFE), Faculty of Sciences Semlalia, Cadi Ayyad University, Marrakesh, Morocco*

(Received 25 June 2022, Accepted 16 September 2022)

Cooling enhancement by mixed convection in a tilted enclosure heated on one wall and vented by injection or suction imposed flows with Alumina-water nanofluid was analyzed. In this study, the control parameters were the inclination angle, $0° \le \theta \le 90°$, nanoparticles volume fraction, $0 \le \phi \le 0.05$, and the mode of the external flow. The combined effects of the above controlling parameters on heat transfer and fluid flow were examined. The results indicated that adding nanoparticles led to an increase in the average temperature and heat transfer rate in the cavity. Moreover, an enhancement in heat transfer rate was achieved by varying the tilt of the cavity. More specifically, better cooling was achieved at higher inclination angles ($\theta \ge 70°$). Finally, higher heat transfer and better cooling were reached in the suction mode. Quantitatively, for $\phi = 0.05$ and $\theta = 0°$, the fluid mean temperature decreased by about 17% by changing the mode from injection to suction.

Keywords: Mixed convection, Vented cavity, Nanofluid, Suction, Injection, Inclination angle

INTRODUCTION

Investigations of mixed convection involving fluids confined in inclined and vented cavities stem from their importance in many applications such as cooling of electronic components, building thermal design optimization, solar power collectors, nuclear reactors, chemical processes, heat exchangers, *etc*. [1-2]. However, the cooling process involving heat transfer fluids is hampered by their low thermal conductivities. Therefore, different methods have been developed to enhance the thermal performance of the working fluids. The suspension of evenly dispersed nano-sized particles in a base fluid to obtain a mixture known as nanofluid is one of the techniques used to enhance the thermal performance of base fluids (water, ethylene glycol (EG), and oil). In many previous studies, it has been demonstrated that nanofluids have a much higher thermal conductivity than pure fluids [3]. Comparative studies involving the addition of different types of nanoparticles have shown an advantage in favor of alumina-based nanofluids in terms of thermal efficiency, which paves the way for more efficient heat transfer applications [4-5]. However, market adoption of nanofluids will only be achieved by overcoming numerous barriers, which are mostly interdependent and can influence each other. Rashidi *et al*. [6] reported that the use of intelligent techniques made it possible to model, with high accuracy, the thermal conductivity of water-EG-based nanofluids with aluminum oxide (Al_2O_3) particles. On a commercial scale, the problem of long-term stability is identified as the main driver for efficient implementation with high precision [7]. Another study showed that the development in temperature resulted in a decrease of more than 80% in viscosity for all nanofluids and that the increase in the nanoparticles volume

*Corresponding author. E-mail: ismail.arroub@usms.ma

concentration clearly improved the dynamic viscosity [8]. On the other hand, Goharshadi *et al*. [9] revealed that at lower shear rates, both EG and nanofluids behaved as non-Newtonian fluids while at greater shear rates, they behaved as Newtonian fluids. Eventually, due to the altered viscosity of fluids and their thermal conductivity, nanofluids are treated abnormally when some nanoparticles are present in the fluid [10-12].

A large number of studies have attempted to investigate natural convection in cavities with variable thermal boundaries using nanofluids. In the case of total heating, Abu-Nada and Oztop [13] investigated natural convection in a cavity with differential heating filled with Cu-water nanofluid and tilted relative to the horizontal plane. Their findings revealed that the heat transfer rose roughly linearly by increasing the Rayleigh (Ra) number. The effect of nanoparticles concentration on Nusselt number was found to be more noticeable at low values of Ra. In addition, the most deterioration of heat transfer was obtained at $\theta = 90°$, but the tilt angle was found to be a useful control variable for pure fluid and nanofluid-filled enclosures. For the same configuration, Kefayati *et al*. [14] investigated water/SiO_2 nanofluid considering different Ra numbers and A of a horizontal enclosure. They reported that the effect of nanoparticles on heat transfer intensified by increasing the A of the enclosure. Alloui *et al*. [15] studied natural convection subjected to heating and cooling uniform by a heat flux and in a shallow rectangular enclosure with a nanofluid. They showed that the convective heat transfer improved at low Ra numbers by increasing the concentration of nanoparticles. Cu-water nanofluid heat transfer by natural convection was examined by Mahmoodi *et al*. [16] in a square enclosure. The obtained results indicated that the Nu of the heat source rose by increasing the Ra numbers and the concentration of nanoparticles. Furthermore, it was observed that maximum and minimum rates of heat transfer were achieved for particular combinations of Ra numbers, heat sink design, and nanofluid type. Other studies have used variable heating. For example, Oztop *et al*. [17] analyzed the heat transfer inside a tilted enclosure loaded with CuO-water-based nanofluids. They concluded that adding CuO improved heat transfer and that the rate of increase was important at low Ra numbers for which conduction prevailed. Recently, the focus has shifted to interior or outside heating using solid bodies of different shapes. In this regard, Aminossadati and Ghasemi [18] investigated conjugate natural convection in an inclined cavity with an Ethylene Glycol-copper nanofluid by enclosing a centered conducting block. Their findings indicated the positive effect of the nanofluid and the size of the block on the heat transfer rate. Based on the results, the transmission of heat was improved by raising the tilt angle, especially at high Ra numbers. Garoosi *et al.* [19] investigated the natural convection within a square cavity filled with nanofluids and equipped with isothermal coolers and heaters. They observed that increasing the number of HACs rather than their size boosted the heat transfer rate more efficiently.

Research on the thermal behavior of nanofluids in a forced convection regime has mainly involved tubular geometries. For instance, Heris *et al*. [20] experimentally investigated the laminar forced convection in a tube heated by a constant temperature using Al_2O_3-water nanofluid. According to the findings, the increase in the Pe number and volume fraction of Al_2O_3 improved the heat transfer coefficient of nanofluids. Demir *et al*. [21] investigated the numerical flow of nanofluids, containing TiO_2 and Al_2O_3 nanoparticles, induced by convection in a horizontal duct with constant wall temperature. The results showed that nanofluids with a high concentration of nanoparticles promoted heat transfer and caused a greater pressure drop. The case of laminar forced convection flow of water-Al_2O_3 nanofluid in a circular tube with homogeneous heat flux was investigated by Bianco *et al*. [22]. They observed higher heat transfer coefficients and lower wall shear stresses in temperature-dependent models. In addition, the promotion of heat transmission involved an increase in either the Reynolds number or particle volume concentration, but, unfortunately, this improvement was always accompanied by the shear stress. Minea [23] studied a fully developed flow of a water-based alumina nanofluid within the horizontal tube insulated from one zone and submitted on the remaining zone to a homogeneous heat flux. The results obtained by three models from the literature expressing λ_{nf} were compared. Comparative results showed uncertainties concerning the properties of the nanofluids used.

Nanofluids mixed convection in rectangular enclosures has been extensively studied due to its many industrial applications. In this regard, Talebi *et al*. [24] studied mixed

convection within a lid-driven enclosure with differential heating completed by the Cu-H_2O. The obtained results indicated that the addition of Cu improved the heat exchange. In addition, they examined the effect of the volume concentration on the distribution of temperature in the enclosure. The same configuration inclined with respect to the horizontal plane was studied by Abu Nada and Chamkha [25], who observed considerable improvement by adding nanoparticles. They reported that such behavior was amplified by the disposition of cavity for average and important values of the Ri number. Muthtamilselvan *et al*. [26] investigated mixed convection within a lid-driven enclosure filled with nanofluids. The cavity was insulated from its vertical sides but heated in the top moving wall. The results were discussed in relation to a wide range of the As and concentrations of nanoparticles, confirming a linear relation between the solid volume percentage. Nu. Salahi *et al*. [27] considered the same configuration with a slight variation of the tilt angle (between 0° and 30°), the same working nanofluid, and an aspect ratio equal to 10. Their findings revealed a quick increase in the Nu for a flow pattern controlled by natural convection. The same issue was addressed by Mansour *et al*. [28], who considered four types of nanoparticles under partial heating from below and total isothermal cooling from its vertical and upper horizontal walls. The effect of the governing parameters (*e.g*., the location of the heating source) on the fluid temperature, fluid flow, and average Nusselt number were examined. The findings showed that larger/(smaller) values of the Nusselt number were achieved by increasing Al_2O_3/(TiO_2).

Mixed convection in ventilated cavities with nanofluids remains less documented compared to lid-driven enclosures despite the importance of the latter in several practical applications. On this topic, Shahi *et al.* [29] conducted an analysis of the mixed convection of copper-water in a ventilated enclosure subjected to applied heated flux. According to their findings, an improvement in the concentration of nanoparticles simultaneously improved Nu and reduced median volume temperature. A similar study was done by Mehrizi *et al.* [30], who focused on various outlet port positions in the presence of a heating obstacle centrally located within the cavity. The results were discussed for different Ris and positions of cavity openings following the increase in the concentration of nanoparticles in heat transfer rate. Selimefendigil and Öztop [31] studied mixed convection in a vented square enclosure with a circling tube isothermally heated from both horizontal walls. The results showed a significant rise in the heat transfer rate when the rotation angle cylinder was increased clockwise. Arroub *et al*. [32-34] investigated mixed convection heat transfer of alumina-H_2O nanofluid in a ventilated enclosure due to injection/(sucking) of incoming/(outgoing) flow for different types of heating. The addition of nanoparticles was found to affect positively the heat transfer, but it led to a rise in the average temperature of the enclosure. Moreover, it was found that the sucked fluid mode resulted in better cooling within the cavity.

The objective of the present study was to perform a numerical simulation of the mixed convection heat transfer inside an inclined ventilated rectangular cavity operating in the suction or injection mode of alumina-water nanofluid flow. The study focused mainly on the identification of the optimal situations that could maximize heat exchange through the nanofluid and the enclosure.

PROBLEM DESCRIPTION AND MATHEMATICAL FORMULATION

Problem Definition

The geometry considered is depicted in Fig. 1. It is a vented enclosure with $A = L'/H' = 2$, tilted by an angle (θ), and heated from the lower wall with a constant temperature. The remaining solid boundaries of the cavity were insulated. The cold Al_2O_3-water nanofluid was admitted from the inlet by injection (Fig. 1a) or leaves the cavity by suction at the outlet (Fig. 1b). We assumed that the alumina and water were in local heat balance and without slipping. The mixture was incompressible and Newtonian, and the flow was laminar and two-dimensional. The parameters of the solid phase (Al_2O_3) and the base fluid (water) were taken at ($T' = 25$ °C) [15]. Except for the density in the buoyancy component, which followed the Boussinesq approximation, the characteristics of nanofluids were also assumed to be stable.

Mathematical Modeling

The nanofluid effective physical properties were obtained using the following equations [14]:

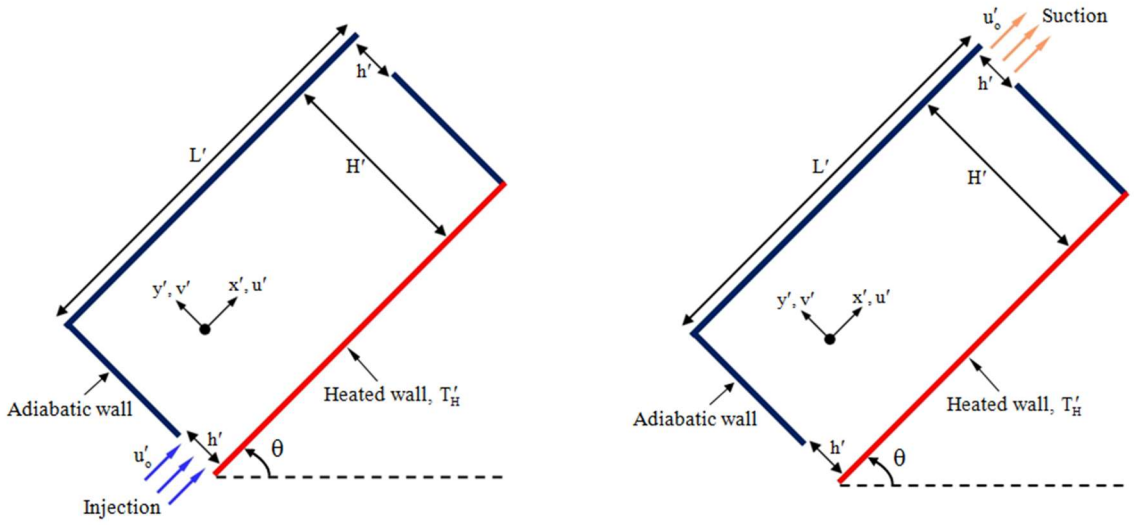

a) Injection mode **b)** Suction mode

Fig. 1. Graphic view of the problem.

$$\rho_{nf} = \phi\rho_s + (1-\phi)\rho_f \tag{1}$$

$$\alpha_{nf} = \frac{\lambda_{nf}}{(\rho c_p)_{nf}} \tag{2}$$

$$(\rho c_p)_{nf} = \phi\,(\rho c_p)_s + (1-\phi)\,(\rho c_p)_f \tag{3}$$

$$(\rho\beta)_{nf} = \phi\rho_s\,\beta_s + (1-\phi)\rho_f\beta_f \tag{4}$$

The effective thermal conductivity of the nanofluid was in good approximation proposed by Hamilton and Crosser [35], commonly used in the literature with the assumption of spherical nanoparticles:

$$\frac{\lambda_{nf}}{\lambda_f} = \frac{\lambda_s + (m-1)\lambda_f - (m-1)\phi\,(\lambda_f - \lambda_s)}{\lambda_s + (m-1)\lambda_f + \phi\,(\lambda_f - \lambda_s)} \tag{5}$$

In this equation, m is the empirical form factor defined by m = 3/s, where s represents the particle sphericity (in the present study, s = 1). The model given by Eq. (5) has been used in numerous previous studies [36-39].

The viscosity (μ_f) of the water and a dilute suspension of small spherical particles (low volume percentage) were utilized to compute the effective dynamic viscosity of nanofluids. According to the Brinkman model [35], the viscosity is calculated as follows:

$$\mu_{nf} = \frac{\mu_f}{(1-\phi)^{2.5}} \tag{6}$$

Under the previous assumptions and using the stream function-vorticity formulation, the dimensionless governing equations were obtained in the following forms:

$$\frac{\partial\Omega}{\partial t} + u\frac{\partial\Omega}{\partial x} + v\frac{\partial\Omega}{\partial y} = \frac{Ra}{Re^2\,Pr}\left[\left(\frac{\varphi}{\left((1-\phi)\,\frac{\rho_f}{\rho_s}+\phi\right)}\right)\frac{\beta_s}{\beta_f} + \frac{1}{\left(\frac{\phi\,\rho_s}{(1-\phi)\,\rho_f}+1\right)}\right]\left(\cos\theta\frac{\partial T}{\partial x} - \sin\theta\frac{\partial T}{\partial y}\right) + \frac{1}{Re}\left[\frac{1}{(1-\phi)^{2.5}\left(\phi\frac{\rho_s}{\rho_f}+(1-\phi)\right)}\right]\left(\frac{\partial^2\Omega}{\partial x^2} + \frac{\partial^2\Omega}{\partial y^2}\right) \tag{7}$$

$$\frac{\partial T}{\partial t} + u\,\frac{\partial T}{\partial x} + v\,\frac{\partial T}{\partial y} = \frac{1}{Re\;Pr}\left(\frac{\frac{\lambda_{nf}}{\lambda_f}}{(1-\phi) + \phi\,\frac{(\rho c_p)_s}{(\rho c_p)_f}}\right)\left(\frac{\partial^2 T}{\partial x^2} + \frac{\partial^2 T}{\partial y^2}\right) \tag{8}$$

$$\frac{\partial^2\Psi}{\partial x^2} + \frac{\partial^2\Psi}{\partial y^2} = -\Omega \tag{9}$$

The dimensionless components of velocity were associated with non-dimensional vorticity and stream function as follows:

$$u = \frac{\partial\Psi}{\partial y} \quad , \quad v = -\frac{\partial\Psi}{\partial x} \quad , \quad \Omega = \frac{\partial v}{\partial x} - \frac{\partial u}{\partial y} \tag{10}$$

Boundary Conditions

The dimensionless hydrodynamic and thermal boundary conditions related to the present study included the

following:

$T = 1$ (for the heated wall)

$u = 0$ and $v = 0$ (for the rigid walls)

$\frac{\partial T}{\partial n} = 0$ (for the adiabatic walls)

$\Psi = 0$ (in the walls under the openings)

$\Psi = B$ (in the remaining rigid walls)

● n denotes normal to the regarded to the adiabatic wall.

The boundary conditions for the injection and suction modes were as follows:

The injection mode:

$T = 0$; $u = 1$; $v = 0$; $\Omega = 0$ and $\Psi = y$ in the entrance opening

The suction mode:

$T = 0$ in the entrance opening

$\Psi = y - (1 - B)$; $u = 1$; $v = 0$ and $\Omega = 0$ in the exit opening

The unknown boundary conditions at the entrance or the exit of the cavity depend on the flow mode. They are extrapolated at each time step by the zero second derivatives consideration of these variables.

The following approximate equation, proposed by Woods [40], was used to assess the stability and accuracy of the unknown vorticity on the rigid walls:

$$\Omega_{\omega} = -\frac{1}{2}\Omega_{\omega+1} - \frac{3}{\Delta\eta^2}\left(\Psi_{\omega+1} - \Psi_{\omega}\right) \tag{11}$$

where ω refers to the wall and Δη corresponds to the spatial step in the latter normal orientation.

HEAT TRANSFER

In a steady state, the dimensionless averaged heat transport rate through the hot side is determined by integration of the local Nusselt number using Simpson's rule. The expression used for the averaged Nusselt number was as follows:

$$Nu = -\frac{1}{A}\left(\frac{\lambda_{nf}}{\lambda_f}\right)\int_0^A \left.\frac{\partial T}{\partial y}\right|_{y=0} dx \tag{12}$$

NUMERICAL PROCEDURE AND TESTS OF VALIDATION

Equations ((7)-(9)) were discretized using the finite difference method. A second-order central difference technique was used to approximate the diffusive terms. Moreover, the advection conditions were discretized employing the differences of second-order upwind approach to eliminate eventual instabilities that are common to such problems. The alternating-direction implicit (ADI) method was used to integrate Eqs. (7) and (8). For the grid 201 × 101 used in this study, stream function values for each grid point were determined at each time step using Eq. (9) and the point successive over-relaxation (PSOR) method. Since the formulation Ψ-Ω was used, the velocities components at each node were calculated using Eq. (10) and updated stream function values.

The validation of the numeric code used was carried out by comparing our findings to those acquired experimentally by Ho *et al.* [41], who studied natural convection with a differential heating square cavity (L′ = H′ = 80 mm) filled with alumina-water. A comparison of results in terms of mean Nusselt numbers is presented in Table 1. The

Table 1. Validation of the Numeric Code Using the Mean Nusselt Number, Nu of the Active Wall

Ra	This study		Ho *et al*. [41] (experimental)		Deviation in %	
	$\phi = 0$	$\phi = 0.001$	$\phi = 0$	$\phi = 0.001$	$\phi = 0$	$\phi = 0.001$
2×10^7	18.83	21.49	18.05	20.5	4.32	4.83
6×10^7	24.16	29.01	23.12	27.6	4.5	5.11
10^8	27.07	31.66	25.85	30.07	4.71	5.29

comparison shows a satisfactory agreement with a maximum difference of about 5.3%. Additional tests of validation were carried out by systematically checking the energy balance of the system at each numerical code execution. As a result, the total amount of heat supplied to the nanofluid by the active wall was compared to the quantity of heat exchanged through the openings of the cavity. The energy balance was fulfilled within 2% of maximum difference.

GRID REFINEMENT EFFECT

A grid size was selected and the tests of grid effect were performed using uniform grids of 201 × 101 and 321 × 161. The comparative results in Table 2 show that the maximum relative deviations generated are lower than 0.97% and 1.67%, respectively, in terms of Ψ_{max} and Nu. Consequently, the grid of 201 × 101 was considered fit to accurately model the problem.

RESULTS AND DISCUSSION

Rayleigh and Reynolds numbers remained steady at 10^6 and 200, respectively. These values led to a value of Ri = 4.03, characterizing the regime of mixed convection.

The aspect ratio of the cavity was fixed at A = 2. The effect of the remaining controlling parameters, such as the volume fraction of nanoparticles, the inclination angle, and the mode of forced flow, were studied, and their effects on the fluid flow, the cooling efficiency, and the temperature distribution were investigated.

Figures 2a-2c illustrate the streamlines and isotherms at different inclination angles in the injection mode with a base fluid ($\phi = 0$, the solid lines) and a nanofluid ($\phi = 0.05$, dashed lines). When the cavity was disposed horizontally ($\theta = 0°$), the streamlines revealed the presence of a large closed cell (Fig. 2a). Due to the shear effect, this large trigonometric cell occupied the whole area over the open lines. When the concentration (ϕ) of the nanoparticles increased from 0 to 5%, the flow structure showed a relatively limited qualitative change. At the level of the hot wall, isotherms were tightened, confirming an efficient convective heat transfer. The presence of a large available area inside the enclosure to the constant coldest temperature was the result of an interaction between the isothermal wall and the nearest open lines. The heat transferred to the latter was directly transferred to the exit by the forced flow. This means that a part of the open lines and the remaining space above these lines stayed thermally unaffected by the presence of the heating plate. Furthermore, at the right part of the cavity, noticeable deviations were observed between the isotherms corresponding to the pure fluid and the nanofluid. This means that the addition of nanoparticles clearly affected the thermal behavior of the flow. Increasing the inclination θ up to 45° and 90° (Figs. 2b-2c) appeared to support the closed cell. Moreover, the thickness of the thermal boundary layer decreased; such behavior is justified by the growing thermal exchange between the active walls with cooling nanofluids caused by the growing effects of the buoyancy forces

Table 2. The Grid Impact of Various Values of ϕ and θ on Two Modes

Injection flow	$\theta = 30°$				$\theta = 60°$			
	$\phi = 0.025$		$\phi = 0.05$		$\phi = 0.025$		$\phi = 0.05$	
	Ψ_{max}	Nu	Ψ_{max}	Nu	Ψ_{max}	Nu	Ψ_{max}	Nu
201 × 101	0.286	15.870	0.286	16.396	0.289	17.444	0.289	17.986
321 × 161	0.288	16.109	0.288	16.633	0.290	17.735	0.290	18.287
Suction flow	$\theta = 0°$				$\theta = 45°$			
	$\phi = 0.025$		$\phi = 0.05$		$\phi = 0.025$		$\phi = 0.05$	
	Ψ_{max}	Nu	Ψ_{max}	Nu	Ψ_{max}	Nu	Ψ_{max}	Nu
201 × 101	0.309	14.738	0.309	15.334	0.318	18.563	0.318	19.161
321 × 161	0.312	14.724	0.312	15.332	0.321	18.516	0.321	19.128

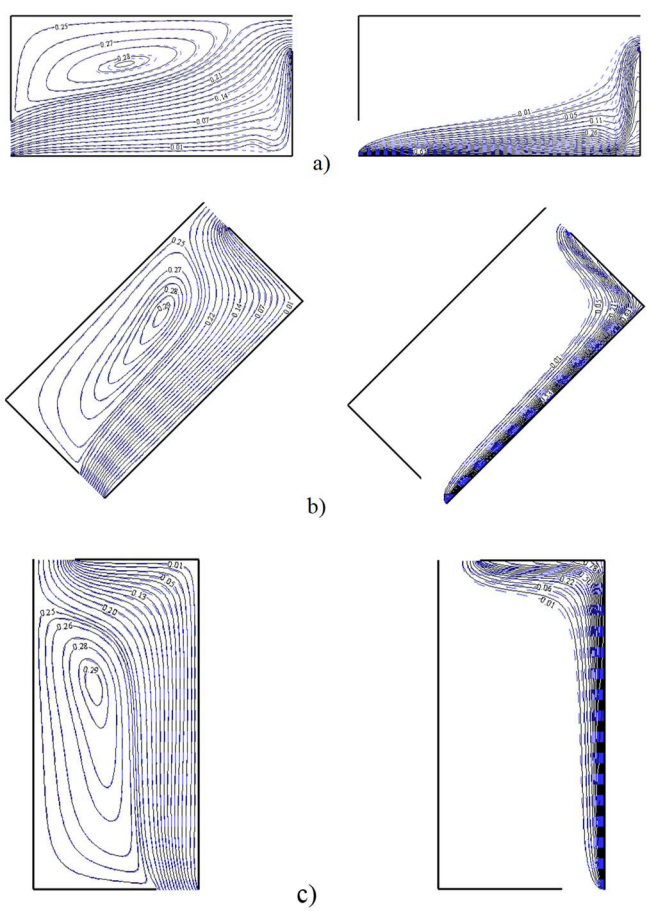

Fig. 2. Streamlines and isotherms for $\phi = 0$ (—) and $\phi = 0.05$ (- - -) in the injection mode at different values of θ : a) $\theta = 0°$, b) $\theta = 45°$, and c) $\theta = 90°$.

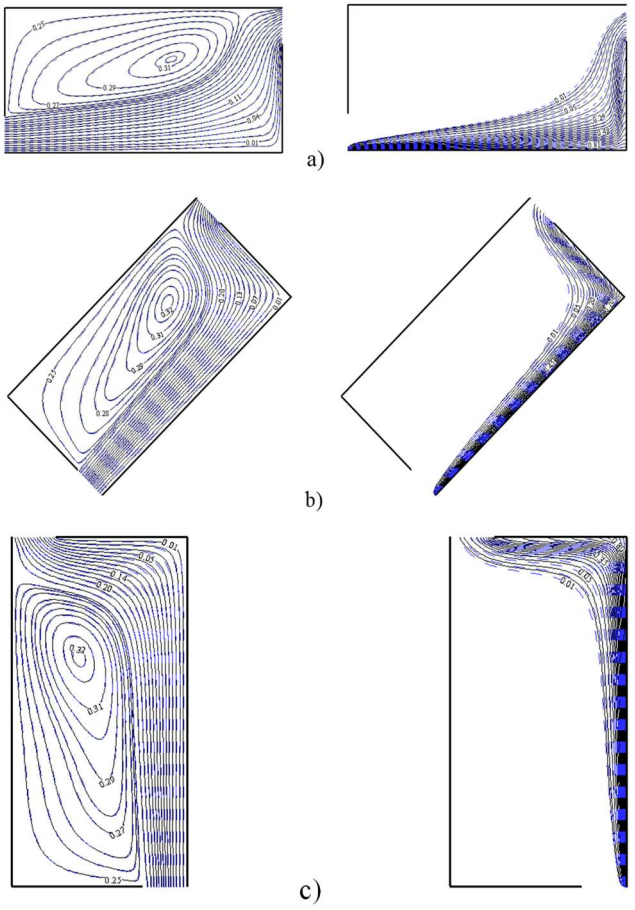

Fig. 3. Streamlines and isotherms for $\phi = 0$ (—) and $\phi = 0.05$ (- - -) in the suction mode at different values of θ: a) $\theta = 0°$, b) $\theta = 45°$, and c) $\theta = 90°$.

favored by the inclination angle. However, it is to mention that for the specified values of θ, the dynamical and thermal structures were seen to be less sensitive to the addition of nanoparticles.

For the suction mode, the effects of the inclination angle on the thermal and dynamical fields are depicted in Figs. 3a-3c in relation to streamlines and isotherms for $\phi = 0$ and $\phi = 0.05$. Under the shear effects, the streamlines for $\theta = 0°$ (Fig. 3a) demonstrated the presence of a large trigonometric cell that occupies almost the above portion of the enclosure and is situated above the open lines of the imposed flow. Compared to the injection mode, this cell was larger in size and intensity. The corresponding isotherms above the heating wall were denser and formed a thinner thermal boundary layer compared to that in the injection mode. This tightening of the isotherms caused a reduction in the size of the thermally active area and, consequently, led to a large cold inactive region on the reminder space inside the cavity. Also, the dynamical and thermal patterns were found not to be affected by the inclusion of nanoparticles. Increasing θ to 45° and 90° (Figs. 3b-3c) resulted in globally similar changes to those evoked for the injection mode (thermal boundary layer thinning, increased size of the closed cell, and cold zone widening). Such behavior can be explained by the growth of the natural convection impact supported by the increase in θ.

Deviations of the average Nu, compared to the tilt angle evaluated on the heated wall, are illustrated in Fig. 4 with various values of ϕ. Globally, an increase in Nu following an

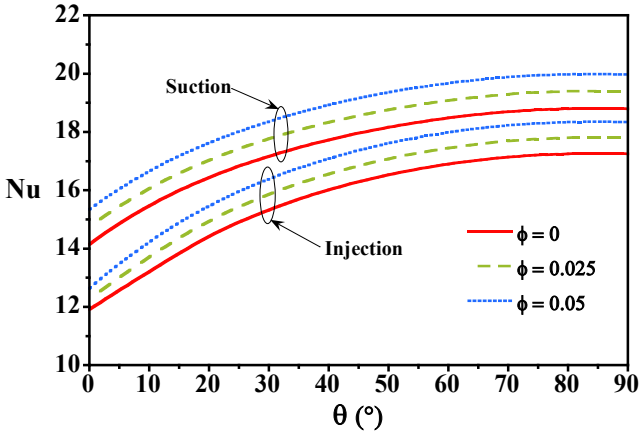

Fig. 4. Variations of Nu *vs*. θ for different values of ϕ.

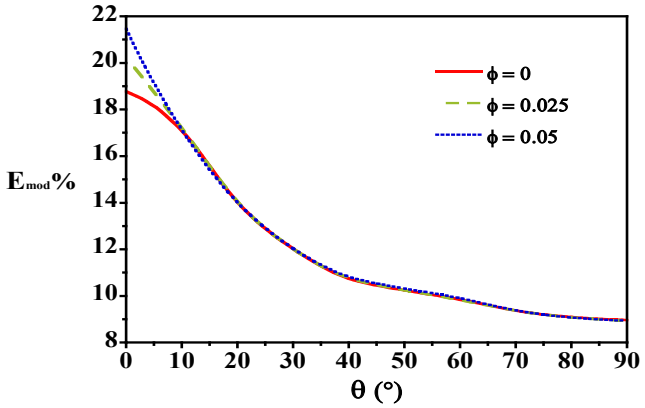

Fig. 5. Variations of E_{mod} *vs*.θ for different values of ϕ.

increase in θ was observed for both injection and suction modes. It is worth noting that the growth in the Nu following the increase in θ was fairly restricted to the range of $0° \le \theta \le 75°$. Above this range, Nu increases barely with an increase in θ, and its growth rate is considerably reduced. The improvement of heat transfer can be attributed to the tremendous interaction between the forced and natural convection, characterized by the development of a thermal boundary layer thickness accompanying the increase in θ (see Figs. 2-3). The increase in ϕ up to 0.05, with a given value of θ, supported Nu in both modes (*i.e*., injection and suction), since the increased effective thermal conductivity of nanofluids resulted from the increase in ϕ. Quantitatively, in both modes and $\theta = 60°$, an improvement of about 6.4% was observed in Nu when the value of ϕ was increased from 0 to 0.05. Compared to the injection mode, the suction mode provided a better heat performance since it enhanced the heat transfer rate in the whole range of θ whether a cavity was filled by water or nanofluid.

To quantify the improvements in the heat transfer based on a comparison between the suction mode and the injection one, variations *vs*. θ of the parameter $E_{mod} = [(Nu_{suction} - Nu_{injection}) / Nu_{injection}] \times 100$ are displayed in Fig. 5. As shown in this figure, the suction mode prevails on the injection mode in the whole range of θ in the presence or in the absence of nanoparticles. The improvement recorded reached its maximum for a horizontal cavity ($\theta = 0°$) supported by the addition of nanoparticles. More precisely, for $\theta = 0°$ and $\phi = 0.05$, for instance, Nu rises from 12.63 to 15.34 by switching from the injection to the suction mode. This corresponded to a relative improvement of about 21.46% in heat exchange. In the case of pure water ($\phi = 0$), this improvement was about 18.77%. As the angle of inclination increased, the parameter E_{mod} undergoes a deterioration with different rates, depending on the range of θ. This behavior was driven by the increased heat exchange corresponding to the increase in θ in injection mode. This can be attributed to the cooperating effects of buoyancy and inertial forces promoted by the increase in the inclination angle, particularly for the injection mode. However, it must be noted that with the addition of alumina to the water, the increase in the heat exchange in the suction mode, compared to the injection one, was visible only in a limited range of θ ($0° \le \theta \le 10°$). Outside this range of θ, the effect of the concentration of alumina on the parameter E_{mod} became negligible. Finally, it should be added that even for the highest value of θ, the increase in the heat transfer in favor of the suction mode remained significant (about 8.9%). This confirms the ability of this mode of ventilation to release better thermal efficiencies for certain vented systems.

The effect of the inclination of the cavity on the fluid mean temperature $\overline{T}$ is exemplified in Fig. 6 for both ventilation modes and different values of ϕ. Figure 6 demonstrates that the parameter $\overline{T}$ decreased sharply reduced by increasing the inclination angle in the range $0° \le \theta \le 30°$ for both suction and injection modes in the presence (nanofluid) and absence (pure water) of

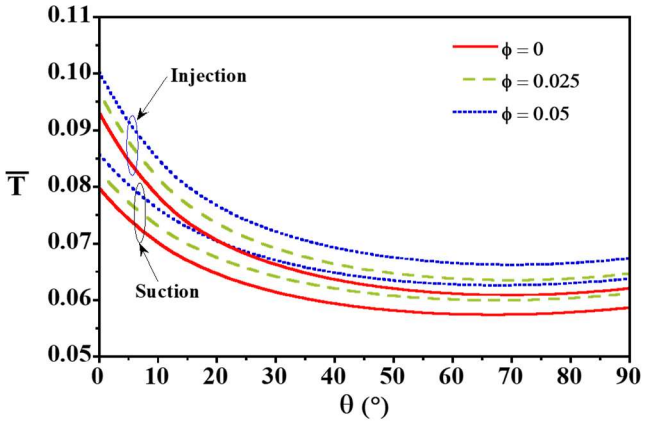

Fig. 6. Variations of $\overline{T}$ *vs.* θ for different values of ϕ.

nanoparticles. This decrease in $\overline{T}$ continues with a lower slope until reaching its minimum values for a critical value of about θ ≈ 70°. This can be attributed to the fact that the increase of θ favors the cooperating effects of forced and natural convection, leading to more heat evacuation and consequently more effective cooling of fluid inside the enclosure. Above this threshold of θ, $\overline{T}$ was less affected by the variations in the inclination angle. For both modes of ventilation and a given θ, the rise in the volume fraction of the nanoparticle increased fluid mean temperature. The suction mode, in comparison with the injection mode, was found to be more efficient in cooling the enclosure because it led to reduced values of $\overline{T}$. Quantitatively, for ϕ = 0.05 and θ = 0°, a decrease of about 17% in $\overline{T}$ was achieved by switching from the suction mode to the injection mode.

CONCLUSIONS

The mixed convection of Al_2O_3-water nanofluids with an inclined ventilated rectangular enclosure with two ports was investigated numerically for two types of imposed external flows. Based on the results, the following conclusions can be drawn:

- The flow pattern consists of a closed cell filling the space not covered by the open streamlines whereas the thermal interaction of the heated wall and the nanofluid was restricted to a limited area close to the former, within which the thermal boundary layer developed. Both streamlines and isotherms undergo limited qualitative changes by varying the control parameters.
- The suction mode was found to be thermally, but not dynamically, more powerful than the injection mode.
- The addition of nanoparticles promotes the heat transfer between the active wall and the nanofluid and augments $\overline{T}$ in the enclosure for the two modes considered.
- The enhancement of Nu was accompanied by a decrease in $\overline{T}$ while increasing θ up to 70°.
- The suction mode significantly improved the rate of heat exchange and was a better ventilation mode, specifically for low values of θ, compared to the injection mode.

Nomenclature

A	Aspect ratio of the cavity $(= L'/H')$
B	Relative height of the openings $(= h'/H')$
c_p	Specific heat (J kg^{-1} K^{-1})
g	Gravitational acceleration (m s^{-2})
h'	Height of the openings (m)
H'	Height of the cavity (m)
L'	Length of the cavity (m)
Nu	Average Nusselt number
Pr	Prandtl number $(= \nu_f/\alpha_f)$
Ra	Rayleigh number $(= g\beta_f(T'_H - T'_C)H'^3/\alpha_f\nu_f)$
Re	Reynolds number $(=u'_oH'/\nu_f)$
Ri	Richardson number $(=Ra/Re^2 Pr)$
t	Dimensionless time $(=t'u'_o/H')$
T	Dimensionless temperature $(=(T'-T'_C)/(T'_H-T'_C))$
T'	Ddimensional temperature (K)
$\overline{T}$	Dimensionless average temperature
T'_C	Temperature of the imposed inflow (K)
T'_H	Dimensional hot temperature (K)
u'_o	Velocity of the imposed flow (m/s)
(u, v)	Dimensionless velocity components $(=(u',v')/u'_o)$
(x, y)	Dimensionless coordinates $(=(x', y')/H')$

Greek symbols

α	Thermal diffusivity (m^2 s^{-1})
β	Thermal expansion coefficient (K^{-1})
θ	Inclination angle of the cavity (°)
λ	Thermal conductivity (W K^{-1} m^{-1})
μ	Dynamic viscosity (N s m^{-2})
ν	Kinematic viscosity (m^2 s^{-1})
ρ	Density (Kg m^{-3})

ϕ Solid volume fraction
Ψ Dimensionless stream function $\left(=\Psi'/u_o'H'\right)$
Ω Dimensionless vorticity $\left(=\Omega' H'/u_o'\right)$

Subscripts

c Cold temperature
f Fluid (water)
H Hot temperature
max Maximum value
min Minimum value
nf Nanofluid
S Solid particles

Superscripts

′ Dimensional variable

REFERENCES

[1] Qasem, N. A.; Abderrahmane, A.; Ahmed, S.; Younis, O.; Guedri, K.; Said, Z.; Mourad, A., Effect of a rotating cylinder on convective flow, heat and entropy production of a 3D wavy enclosure filled by a phase change material. *Appl. Therm. Eng.* **2022**, *214*, 118818. DOI: 10.1016/j.applthermaleng.2022.118818.

[2] Bhatti, M. M.; Riaz, A.; Zhang, L.; Sait, S. M.; Ellahi, R., Biologically inspired thermal transport on the rheology of Williamson hydromagnetic nanofluid flow with convection: An entropy analysis. *J. Therm. Anal. Cal.* **2021**, *144*, 2187-2202. DOI: 10.1007/s10973-020-09876-5.

[3] Esfe, M. H.; Karimipour, A.; Yan, W. M.; Akbari, M.; Safaei, M. R.; Dahari, M., Experimental study on thermal conductivity of ethylene glycol based nanofluids containing Al_2O_3 nanoparticles. *Int. J. Heat and Mass Tran.* **2015**, *88*, 728-734. DOI: 10.1016/j.ijheatmasstransfer.2015.05.010.

[4] Sridhara, V.; Satapathy, L. N., Al_2O_3-based nanofluids: a review. *Nano. Res. Lett.* **2011**, *6*, 456. DOI: 10.1186/1556-276X-6-456.

[5] Sudarmadji, S.; Soeparman, S.; Wahyudi, S.; Hamidy, N., Effects of cooling process of Al_2O_3-water nanofluid on convective heat transfer. *FME Trans.* **2014**, *42*, 155-160. DOI: 10.5937/fmet1402155S.

[6] Rashidi, M. M.; Nazari, M. A., Mahariq, I., Ali, N., Modeling and Sensitivity Analysis of Thermal Conductivity of Ethylene Glycol-Water Based Nanofluids with Alumina Nanoparticles. *Exp. Tech.* **2022**, *16*, 1-8. DOI: 10.1007/s40799-022-00567-4.

[7] Alagumalai, A.; Qin, C.; Vimal, K. E. K.; Solomin, E.; Yang, L.; Zhang, P.; Otanicar, T., Kasaeian, A.; Chamkha, A. J.; Rashidi, M. M.; Wongwises, S.; Ahn. H. S.; Lei, Z.; Saboori, T.; Mahian, O., Conceptual analysis framework development to understand barriers of nanofluid commercialization. *Nano Ener.* **2022**, *92*, 106736. DOI: 10.1016/j.nanoen.2021.106736.

[8] Harchaoui, A.; Mazouzi, R.; Karas, A., The Rheology of Nanolubricants Based on Fe_2O_3, Al_2O_3, and ZnO Oxide Nanoparticles: A Comparative Study. *Phys. Chem. Res.* **2023**, *11*, 181-189. DOI: 10.22036/PCR.2022.328709.2027.

[9] Goharshadi, E. K.; Mahvelati, T.; Yazdanbakhsh, M., Lanthania Colloidal Nanoparticles: Hydrothermal Synthesis, Structural, and Rheological Properties. *Phys. Chem. Res.* **2016**, *4*, 143-151. DOI: 10.22036/pcr.2016.12650.

[10] Rasool, G.; Saeed, A. M.; Lare, A. I.; Abderrahmane, A.; Guedri, K.; Vaidya, H.; Marzouki, R., Darcy-Forchheimer Flow of Water Conveying Multi-Walled Carbon Nanoparticles through a Vertical Cleveland Z-Staggered Cavity Subject to Entropy Generation. *Microm.* **2022**, *13*, 744. DOI:10.3390/mi13050744.

[11] Alshare, A.; Abderrahmane, A.; Guedri, K.; Younis, O.; Fayz-Al-Asad, M.; Ali, H. M.; Al-Kouz, W., Hydrothermal and Entropy Investigation of Nanofluid Natural Convection in a Lid-Driven Cavity Concentric with an Elliptical Cavity with a Wavy Boundary Heated from Below. *Nanom.* **2022**, *12*, 1392. DOI: 10.3390/nano12091392.

[12] Rashid, F. L.; Hussein, A. K.; Malekshah, E. H.; Abderrahmane, A.; Guedri, K.; Younis, O., Review of Heat Transfer Analysis in Different Cavity Geometries with and without Nanofluids. *Nanom.* **2022**, *12*, 2481. DOI: 10.3390/nano12142481.

[13] Abu-Nada, E.; Oztop, H. F., Effects of inclination angle on natural convection in enclosures filled with Cu-water nanofluid. *Int. J. Heat Fluid Flow* **2009**, *30*, 669-678. DOI: 10.1016/j.ijheatfluidflow.2009.02.001.

[14] Kefayati, G. R.; Hosseinizadeh, S. F.; Gorji, M.; Sajjadi, H., Lattice Boltzmann simulation of natural convection in tall enclosures using water/SiO_2 nanofluid.

Inte. Com. Heat and Mass Tran. **2011**, *38*, 798-805. DOI: 10.1016/j.icheatmasstransfer.2011.03.005.

[15] Alloui, Z.; Guiet, J.; Vasseur P.; Reggio, M., Natural convection of nanofluids in a shallow rectangular enclosure heated from the side. *Can. J. Chem. Eng.* **2012**, *90*, 69-78. DOI: 10.1002/cjce.20523.

[16] Mahmoodi, M.; Arani, A. A. A.; Sebdani, S. M.; Nazari S.; Akbari, M., Free convection of a nanofluid in a square cavity with a heat source on the bottom wall and partially cooled from sides. *Ther. Sci.* **2014**, *18*, S283-S300. DOI: 10.2298/TSCI110406011A.

[17] Oztop, H. F.; Mobedi, M.; Abu-Nada E.; Pop, I., A heatline analysis of natural convection in a square inclined enclosure filled with a CuO nanofluid under non-uniform wall heating condition. *Int. J. Heat Mass Tran.* **2012**, *55*, 5076-5086. DOI: 10.1016/j.ijheatmasstransfer.2012.05.007.

[18] Aminossadati S. M.; Ghasemi, B., Conjugate natural convection in an inclined nanofluid-filled enclosure. *Int. J. Num. Meth. Heat & Fluid Flow* **2012**, *22*, 403-423. DOI: 10.1108/09615531211215729.

[19] Garoosi, F.; Bagheri, G.; Talebi, F., Numerical simulation of natural convection of nanofluids in a square cavity with several pairs of heaters and coolers (HACs) inside. *Int. J. Heat and Mass Tran.* **2013**, *67*, 362-376. DOI: 10.1016/j.ijheatmasstransfer.2013.08.034.

[20] Heris, S. Z.; Esfahany, M. N.; Etemad, S. G., Experimental investigation of convective heat transfer of Al_2O_3/water nanofluid in circular tube. *Int. J. Heat and Fluid Flow* **2007**, *28*, 203-210. DOI: 10.1016/j.ijheatfluidflow.2006.05.001.

[21] Demir, H.; Dalkilic, A. S.; Kürekci, N. A.; Duangthongsuk, W.; Wongwises, S., Numerical investigation on the single phase forced convection heat transfer characteristics of TiO_2 nanofluids in a double-tube counter flow heat exchanger. *Int. Com. Heat and Mass Tran.* **2011**, *38*, 218-228. DOI: 10.1016/j.icheatmasstransfer.2010.12.009.

[22] Bianco, V.; Chiacchio, F.; Manca O.; Nardini, S., Numerical investigation of nanofluids forced convection in circular tubes. *App. Ther. Eng.* **2009**, *29*, 3632-3642. DOI: 10.1016/j.applthermaleng.2009.06.019.

[23] Minea, A. A., Uncertainties in modeling thermal conductivity of laminar forced convection heat transfer with water alumina nanofluids. *Int. J. Heat and Mass Tran.* **2014**, *68*, 78-84. DOI: 10.1016/j.ijheatmasstransfer.2013.09.018.

[24] Talebi, F.; Mahmoudi, A. H.; Shahi, M., Numerical study of mixed convection flows in a square lid-driven cavity utilizing nanofluid. *Int. Com. Heat and Mass Tran.* **2010**, *37*, 79-90. DOI: 10.1016/j.icheatmasstransfer.2009.08.013.

[25] Abu-Nada, E.; Chamkha, A. J., Mixed convection flow in a lid-driven inclined square enclosure filled with a nanofluid. *Eur. J. Mech. B/Flui.* **2010**, *29*, 472-482. DOI: 10.1016/j.euromechflu.2010.06.008.

[26] Muthtamilselvan, M.; Kandaswamy, P.; Lee, J., Heat transfer enhancement of copper-water nanofluids in a lid-driven enclosure. *Com. Nonl. Sci. Num. Sim.* **2010**, *15*, 1501-1510. DOI: 10.1016/j.cnsns.2009.06.015.

[27] Salahi, H.; Sharif, M. A.; Rasouli, S., Laminar mixed convective heat transfer in a shallow inclined lid-driven cavity filled with Nanofluid. *J. Ther. Sci. Eng. App.* **2015**, *7*, 041016. DOI: 10.1115/1.4031221.

[28] Mansour, M. A.; Mohamed, R. A.; Abd-Elaziz, M. M.; Ahmed, S. E., Numerical simulation of mixed convection flows in a square lid-driven cavity partially heated from below using nanofluid. *Int. Com. Heat and Mass Tran.* **2010**, *37*, 1504-1512. DOI: 10.1016/j.icheatmasstransfer.2010.09.004.

[29] Shahi, M.; Mahmoudi, A. H.; Talebi, F., Numerical study of mixed convective cooling in a square cavity ventilated and partially heated from the below utilizing nanofluid. *Int. Com. Heat and Mass Tran.* **2010**, *37*, 201-213. DOI: 10.1016/j.icheatmasstransfer.2009.10.002.

[30] Mehrizi, A. A.; Farhadi, M.; Afroozi, H. H.; Sedighi, K.; Darz, A. R., Mixed convection heat transfer in a ventilated cavity with hot obstacle: effect of nanofluid and outlet port location. *Inter. Com. Heat and Mass Tran.* **2012**, *39*, 1000-1008. DOI: 10.1016/j.icheatmasstransfer.2012.04.002.

[31] Selimefendigil, F.; Öztop, H. F., Estimation of the mixed convection heat transfer of a rotating cylinder in a vented cavity subjected to nanofluid by using

generalized neural networks. *Num. Heat Tran., Part A, App.* **2014**, *65*, 165-185. DOI: 10.1080/ 10407782.2013.826109.

[32] Arroub, I.; Bahlaoui, A.; Raji, A.; Hasnaoui, M.; Naïmi, M., Cooling Enhancement by Nanofluid Mixed Convection inside a Horizontal Vented Cavity Submitted to Sinusoidal Heating. *Eng. Comp.* **2018**, *35*, 1747-1773. DOI: 10.1108/EC-03-2017-0080.

[33] Arroub, I.; Bahlaoui, A.; Raji, A.; Hasnaoui, M.; Naïmi, M., Varying Heating Effect on Mixed Convection of Nanofluids in a Vented Horizontal Cavity with Injection or Suction. *Heat Tran. Eng.* **2019**, *40*, 941-958. DOI: 10.1080/01457632.2018.1446876.

[34] Arroub, I.; Bahlaoui, A.; Belhouideg, S.; Raji, A.; Hasnaoui, M., Heat transfer performance in a tilted cavity submitted to external flow of nanofluid. *AIP Conf. Proc.* **2021**, *2345*, 020004. DOI: 10.1063/5.0049447.

[35] Goharshadi, E. K.; Ahmadzadeh, H.; Samiee, S.; Hadadian, M., Nanofluids for Heat Transfer Enhancement-A Review. *Phys. Chem. Res*. **2013**, *1*, 1-33. DOI: 10.22036/PCR.2013.2791.

[36] Alsabery, A. I.; Chamkha, A. J.; Saleh, H.; Hashim, I., Heatline visualization of conjugate natural convection in a square cavity filled with nanofluid with sinusoidal temperature variations on both horizontal walls. *Int. J. Heat and Mass Tran.* **2016**, *100*, 835-850. DOI: 10.1016/j.ijheatmasstransfer.2016.05.031.

[37] Kalidasan, K.; Velkennedy, R.; Kanna, P. R., Natural convection heat transfer enhancement using nanofluid and time-variant temperature on the square enclosure with diagonally constructed twin adiabatic blocks. *Appl. Ther. Eng.* **2016**, *92*, 219-235. DOI: 10.1016/j.applthermaleng.2015.09.077.

[38] Malik, S.; Nayak, A. K., A comparative study of mixed convection and its effect on partially active thermal zones in a two sided lid-driven cavity filled with nanofluid. *Eng. Sci. Tech., Int. J.* **2016**, *19*, 1283-1298. DOI: 10.1016/j.jestch.2016.02.008.

[39] Arroub, I.; Bahlaoui, A.; Ezzaraa K.; Raji, A.; Hasnaoui, M.; Naïmi, M., Effect of Phase Shift on Mixed Convection in a Rectangular Vented Cavity filled with a Nanofluid and Submitted to Periodic Heating. *IOP Conf. Ser.: J. Phy.* **2019**, *1226*, 012001. DOI: 10.1088/1742-6596/1226/1/012001.

[40] Woods, L. C., A note on the numerical solution of fourth order differential equations, *Aero. Quar.* **1954**, *5*, 176-184. DOI: 10.1017/S0001925900001177.

[41] Ho, C. J.; Liu, W. K.; Chang, Y. S.; Lin, C. C., Natural convection heat transfer of alumina-water nanofluid in vertical square enclosures: An experimental study. *Int. J. Ther. Sci.* **2010**, *49*, 1345-1353. DOI: 10.1016/j.ijthermalsci.2010.02.013.